DYNAMIC MODELS IN SUPPORT OF KALMAN FILTER BASED REGISTRATION OF VIDEO IMAGERY

John T. Dolloff, Senior Principal Scientist
InnoVision Basic and Applied Research Office
Sensor Geopositioning Center
National Geospatial-Intelligence Agency (contractor)
12300 Sunrise Valley Dr
Reston, VA 20191
john.t.dolloff.ctr@nga.mil

"This material is based upon work supported by a DoD contract. Any opinions, findings and conclusions or recommendations expressed in this material are those of the author(s) and do not necessarily reflect the views of the Government."

ABSTRACT

The registration of video imagery using a Kalman Filter is important for the subsequent accurate and reliable geolocation of measured objects in the registered image frames. Use of the Kalman Filter is a fairly recent yet common approach to near real-time video registration in the geopositioning community. Key to optimal Kalman Filter performance is the Kalman Filter state prediction process between measurement updates. This process propagates the state vector and its error covariance across the corresponding time interval and is based on an underlying dynamic model. The Kalman filter state vector usually includes corrections to a supplied reference trajectory (meta-data), hence, the underlying dynamic model must statistically describe reference trajectory error. This error is reasonably assumed bounded with nearly constant variance (uncertainty) and decaying positive temporal correlation over the registration interval of interest and in the absence of a meta-data drop-out. This paper describes the state vector prediction process and an underlying and recommended dynamic model with the above characteristics. It also presents corresponding performance based on the simulation of 8000 frames of video EO imagery overlaying a constant area of interest. The benefit that tie points bring to the registration process, each assumed measured in most frames and in concert with the recommended dynamic model, is highlighted.

KEYWORDS: Kalman filter, registration, geopositioning, video imagery, dynamic model

INTRODUCTION

The registration of video imagery using a Kalman Filter is important for the subsequent accurate and reliable geolocation of measured objects in the registered image frames. Use of the Kalman Filter is a fairly recent yet common approach to near real-time video registration in the geopositioning community (Taylor, et. al., 2010). Key to optimal Kalman Filter performance is the Kalman Filter state prediction process between measurement updates. This process propagates the Kalman Filter state vector and its error covariance across the corresponding time interval. The measurements on either side of the prediction time interval are usually image measurements of tie points and/or ground control points within the image frames.

The Kalman Filter state vector typically contains corrections to sensor/platform metadata, such as position, velocity, attitude, and attitude rate. Usually the metadata comes into the Kalman Filter as a reference trajectory based upon on-board GPS/INU processing. The reference trajectory contains errors characterized as a multi-variate stochastic process with bounded and relatively constant expected magnitude and specific temporal correlation characteristics. For example, if reference trajectory one-sigma position component error is approximately 10 m at time t, we expect it to be approximately the same value at time $t + 100$ seconds as well, not three times that value, assuming no meta-data drop-out. (We are talking about the expected magnitude of error at a given time, not the actual (realization of) error.) The Kalman Filter dynamic model must capture these error characteristics in a reliable and flexible manner. The Series Gauss-Markov I dynamic model recommended in this paper does so. It is

Approved for Public Release: Case #11-097

described in detail, along with other models more typically employed by the general tracking community which do not capture these characteristics with high fidelity, such as the Gauss-Markov I Velocity and the Integrated Velocity dynamic models.

In addition, this paper presents examples of video image registration using a Kalman Filter and the dynamic models mentioned above. These examples are based on simulated data of a sensor/platform imaging a constant area of interest. Eight thousand overlaying frames of video EO imagery cover the area. The Kalman Filter inputs the reference trajectory to be corrected along with various combinations of tie point and optionally ground control point measurements within the image frames. Note that the availability of the reference trajectory allows for the linearization of the problem and the subsequent application of a linear estimator, in our case, the (extended) Kalman Filter. This also assumes that reference trajectory errors are not extremely large and imaging geometry reasonable.

The Kalman Filter then provides a best estimate of corrections to the reference trajectory as well as a best estimate of tie point 3D ground locations. In addition and in parallel, general ground points are extracted monoscopically using their measured image coordinates in a single frame, the corrected reference trajectory output from the Kalman Filter, and an externally supplied DEM. The paper then compares errors in these various solutions to their accuracy predictions based on the Kalman Filter's error covariance and error propagation. In addition, the substantial benefits that tie points, each assumed measured in most frames, bring to the registration process are demonstrated when used in conjunction with the Kalman Filter and the recommended dynamic model.

The roadmap to the remainder of this paper is as follows: (1) various dynamic models are described mathematically and one recommended for the application of interest, (2) an example of corresponding steady state variance (expected magnitude of error) and temporal correlation associated with the recommended dynamic model is presented graphically, and (3) various registration examples are described and performance results presented graphically. A summary, appendix of underlying equations from linear systems theory, and references conclude the paper.

DYNAMIC MODEL DESCRIPTIONS

State Vector and Kalman Filter Background

We first present a review of the Kalman Filter basic equations. Let X correspond to the $(n \times 1)$ state vector to be estimated, subscript k to the time step corresponding to time t_k, and the superscripts – and + to the propagated best estimate and updated best estimate of the state vector, respectively. Let P correspond to the $(n \times n)$ error covariance matrix of X, Φ the $(n \times n)$ state transition matrix representing the modeled state dynamics, and Q the $(n \times n)$ process noise error covariance matrix representing the uncertainty in the modeled state dynamics. The Kalman Filter propagation equations from time t_k to time t_{k+1} are:

$$X_{k+1}^{-} = \Phi_{k+1} X_k^{+} \tag{1}$$

$$P_{k+1}^{-} = \Phi_{k+1} P_k^{+} \Phi_{k+1}^{T} + Q_{k+1}$$

The Kalman Filter update is based on the difference between the $(m \times 1)$ measurement vector M and the predicted measurement vector M^{-} at time t_k. R is the $(m \times m)$ error covariance matrix for the measurement M and H the partial derivative of M with respect to X. The Kalman Filter measurement update equations are:

$$X_{k+1}^{+} = X_{k+1}^{-} + G_{k+1}(M_{k+1} - M_{k+1}^{-}) \tag{2}$$

$P_{k+1}^{+} = (I - G_{k+1}H_{k+1})P_{k+1}^{-}$, where

$$G_{k+1} = P_{k+1}^{-} H_{k+1}^{T} (H_{k+1} P_{k+1}^{-} H_{k+1}^{T} + R_{k+1})^{-1}$$

See (Gelb, 1974) for a general introduction to Kalman Filters and for further details.

Let us now concentrate on the modeled state dynamics over the time interval $\Delta t = (t_{k+1} - t_k) > 0$, dropping subscripts and superscripts when appropriate for convenience. In particular, let us examine the state transition matrix Φ and the process noise error covariance matrix Q of Equations 1. Furthermore, let us make the reasonable assumption that the state dynamics are independent between the various state component groups of interest, such as those corresponding to sensor position and attitude. Thus, for our current analyses we simply assume that the state X consists only of a "position" component x and its velocity $\dot{x}$, i.e., $n = 2$, and $X = (x \quad \dot{x})^T$, a $(2x1)$ vector.

These components can represent position/velocity of any of the three sensor position component groups or can represent attitude/rate of any of the three sensor attitude component groups. Furthermore, in the application of interest, these components represent corrections to a reference trajectory, and the time t_k associated with frame k. Also, since we are concentrating on only the state dynamics for now, we assume that there are no measurements.

Series Gauss-Markov I Dynamic Model

The baseline state dynamic model that we employ is the Series GM1 model, outlined in Figure 1. The ω correspond to various mean-zero, Gaussian white noise processes and the β to inverse time constants. This dynamic model is given its name because it consists of a cascaded series of two Gauss-Markov I models, one for position and one for velocity. (Note that naming conventions vary; names used in this paper were selected by the author as most descriptive.)

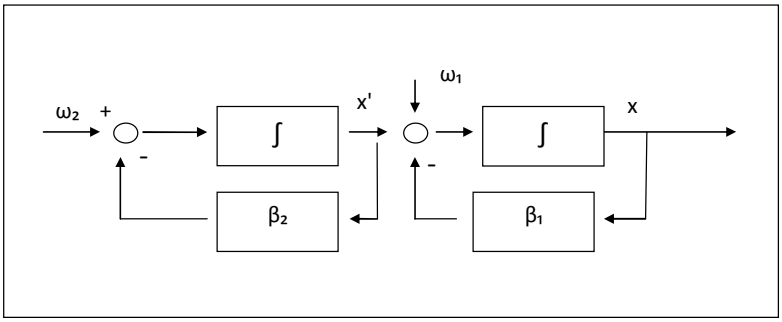

Figure 1. Series GM1 dynamic model process flow.

The corresponding continuous dynamic model for the state is as follows, where the power spectral density for the continuous white noise process ω_1 is $\sigma_{\omega 1}^2$, the power spectral density for the continuous white noise process ω_2 is $\sigma_{\omega 2}^2$, and $W = (w_1 \quad w_2)^T$. Assuming the components of X have units of m and m/s, respectively, $\sigma_{\omega 1}^2$ has units of m^2/s and $\sigma_{\omega 2}^2$ units of m^2/s^3.

$$\dot{X} = \begin{pmatrix} -\beta_1 & 1 \\ 0 & -\beta_2 \end{pmatrix} X + W \tag{3}$$

The above differential equation with respect to time forms the basis for the corresponding discrete state dynamic model for both the state and its covariance.

$$X_{k+1} = \Phi X_k + W_k \tag{4}$$

$$P_{k+1} = \Phi P_k \Phi^T + Q$$

$$\Phi = \begin{pmatrix} e^{-\beta_1 \Delta t} & (\beta_2 - \beta_1)^{-1}\left(e^{-\beta_1 \Delta t} - e^{-\beta_2 \Delta t}\right) \\ 0 & e^{-\beta_2 \Delta t} \end{pmatrix}, \beta_2 \neq \beta_1 \tag{5}$$

$$Q = \begin{pmatrix} Q_{11} & Q_{12} \\ Q_{21} & Q_{22} \end{pmatrix}$$

$$Q_{11} = \sigma_{\omega 2}^2 (\beta_2 - \beta_1)^{-2} \left(0.5\beta_1^{-1}\left(1 - e^{-2\beta_1 \Delta t}\right) + 0.5\beta_2^{-1}\left(1 - e^{-2\beta_2 \Delta t}\right) - 2(\beta_1 + \beta_2)^{-1}\left(1 - e^{-(\beta_1 + \beta_2)\Delta t}\right)\right) + \sigma_{\omega 1}^2 0.5\beta_1^{-1}\left(1 - e^{-2\beta_1 \Delta t}\right)$$

$$Q_{12} = Q_{21} = \sigma_{\omega 2}^2 (\beta_2 - \beta_1)^{-1} \left((\beta_1 + \beta_2)^{-1}\left(1 - e^{-(\beta_1 + \beta_2)\Delta t}\right) - 0.5\beta_2^{-1}\left(1 - e^{-2\beta_2 \Delta t}\right)\right)$$

$$Q_{22} = \sigma_{w2}^2 0.5\beta_2^{-1}\left(1 - e^{-2\beta_2 \Delta t}\right)$$

The Series GM1 dynamic model corresponds to a mean-zero, stochastic process X, and in our application, the error in the reference trajectory, and has a statistically bounded covariance P_k, i.e., $\|P_k\| < \infty$ as $k \to \infty$ or as $\Delta t \to \infty$ for fixed $(k-1)$. In particular, the variances for both the velocity and position components are finite and constant in steady state. The variance and temporal (auto) correlation for each of these components is as follows:

$$E\{x(t)x(t+\Delta t)\} \equiv \sigma_x^2 \rho_x(\Delta t) = \tag{6}$$

$$\sigma_{\omega 2}^2(\beta_2-\beta_1)^{-2}\left(0.5\beta_1^{-1}e^{-\beta_1\Delta t} - (\beta_1+\beta_2)^{-1}e^{-\beta_1\Delta t} + 0.5\beta_2^{-1}e^{-\beta_2\Delta t} - (\beta_1+\beta_2)^{-1}e^{-\beta_2\Delta t}\right) + \sigma_{\omega 1}^2 0.5\beta_1^{-1}e^{-\beta_1\Delta t}$$

$$E\{(\dot{x}(t)\dot{x}(t+\Delta t)\} \equiv \sigma_{\dot{x}}^2 \rho_{\dot{x}}(\Delta t) = \sigma_{\omega 2}^2 0.5\beta_2^{-1}e^{-\beta_2\Delta t}$$

The operator E corresponds to expected value. The steady state variance for position and velocity are σ_x^2 and $\sigma_{\dot{x}}^2$, respectively. The functions ρ_x and $\rho_{\dot{x}}$ are strictly positive definite temporal correlation functions, both equal to 1 at $\Delta t = 0$.

Gauss-Markov I Velocity Dynamic Model

The Series GM1 dynamic model is also very general. In particular, when $\sigma_{w1}^2 = 0$ and $\beta_1 \to 0$, we obtain the GM1 Velocity dynamic model as depicted in Figure 2 and the following equations:

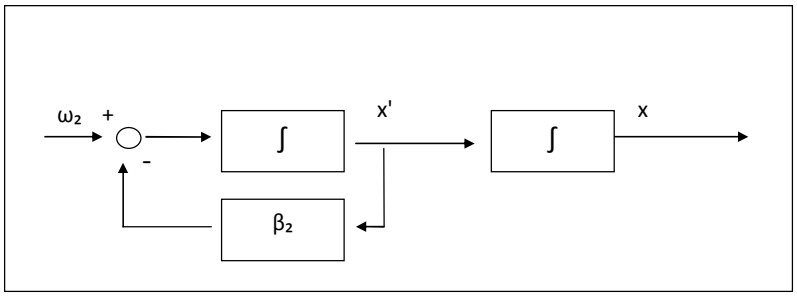

Figure 2. GM1 Velocity dynamic model process flow.

$$\Phi = \begin{pmatrix} 1 & \beta_2^{-1}\left(1-e^{-\beta_2\Delta t}\right) \\ 0 & e^{-\beta_2\Delta t} \end{pmatrix} \tag{7}$$

$$Q = \sigma_{\omega 2}^2 \begin{pmatrix} 0.5\beta_2^{-3}\left(2\beta_2\Delta t - 3 + 4e^{-\beta_2\Delta t} - e^{-2\beta_2\Delta t}\right) & 0.5\beta_2^{-2}\left(1-2e^{-\beta_2\Delta t}+e^{-2\beta_2\Delta t}\right) \\ 0.5\beta_2^{-2}\left(1-2e^{-\beta_2\Delta t}+e^{-2\beta_2\Delta t}\right) & 0.5\beta_2^{-1}\left(1-e^{-2\beta_2\Delta t}\right) \end{pmatrix}$$

This dynamic model has a statistically bounded variance for the velocity component but not for the position component. In other words, the variance of position increases without bound as the time interval Δt or the time index k increases without bound – it is a non-stationary stochastic process.

Integrated Velocity Dynamic Model

In addition, when $\beta_2 \to 0$ as well, the Series GM1 model becomes the Integrated Velocity dynamic model, as depicted in Figure 3 and the following equations:

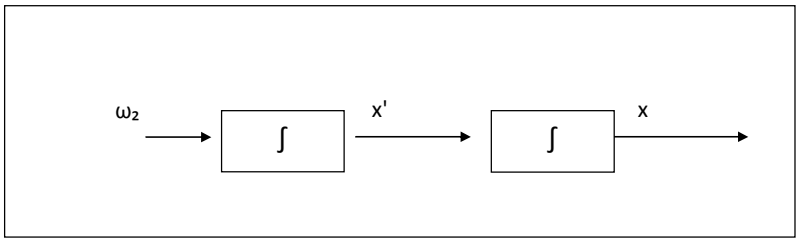

Figure 3. Integrated Velocity dynamic model process flow.

$$\Phi = \begin{pmatrix} 1 & \Delta t \\ 0 & 1 \end{pmatrix} \tag{8}$$

$$Q = \sigma_{\omega 2}^2 \begin{pmatrix} \Delta t^3/3 & \Delta t^2/2 \\ \Delta t^2/2 & \Delta t \end{pmatrix}$$

This dynamic model has unbounded variance for both the velocity and the position components. Again, it is a non-stationary stochastic process. It is a relatively simple and commonly used dynamic model in Kalman Filter tracking applications that typically do not have a reference trajectory available, but do have frequent absolute measurements available, such as those equivalent to image measurements of ground control points.

See the appendix for further details on the derivations of the above dynamic models. (Another interesting dynamic model, "GM2 Position", with bounded 2×2 covariance was not presented above due to space limitations.)

EXAMPLE OF STEADY STATE VARIANCE AND TEMPORAL CORRELATION

In this section of the paper, we present an example of the steady state variance and temporal correlation for the baseline dynamic model, the Series GM1, characterized by the following parameter values:

$T_2 = \beta_2^{-1} = 18\ s, T_1 = \beta_1^{-1} = 12\ s, \sigma_{\omega 2} = 0.5\ m/s^{1.5}\ ,\ \sigma_{\omega 1} = 0\ ,\ \Delta t = 0.1\ s\ ,$ (9)

and initial 2×2 covariance $P_0 = 0$.

Note that these parameter values are "generic" and do not necessarily correspond to a specific sensor/platform.

Figure 4 presents the corresponding position variance (one-sigma) as a function of time based on the implementation of Equations 4 for the state covariance P_{k+1}, i.e., sequential evaluation from $k = 0,1,2,3,...$ Note that position variance corresponds to $P_{k+1}(1,1)$ and that steady state is reached in about 70 seconds, after which the stochastic process is stationary, e.g., the variance is constant. Also, the same steady state value of approximately 14 m one-sigma (standard deviation or square root of variance) is reached no matter the value of the initial condition P_0 since the corresponding dynamic system (Φ and Q) is stable. Figure 5 presents the corresponding position temporal (auto) correlation function. Also, although not shown, velocity variance reaches steady state as well, a one-sigma value of approximately 1.5 m/s reached in about 45 seconds. Its temporal (auto) correlation function is similar to that for position, but is strictly a single decaying exponential per Equations 6. The values of β (inverse time constants) dictate the shape of the correlation curves.

(As a further note of interest, since we are dealing with linear time-invariant systems (see appendix), we get the same end results for both X and P if we implement Equations 4 for $k = 0,1,2,..,n$ using time interval Δt, as if we implement Equations 4 for $k = 0,1,..,n/m$ using time interval $m\Delta t$.)

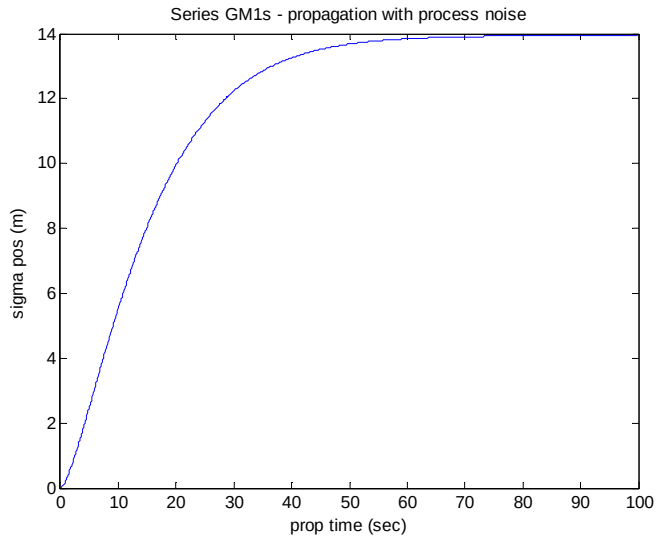

Figure 4. Series GM1 position one-sigma vs. time.

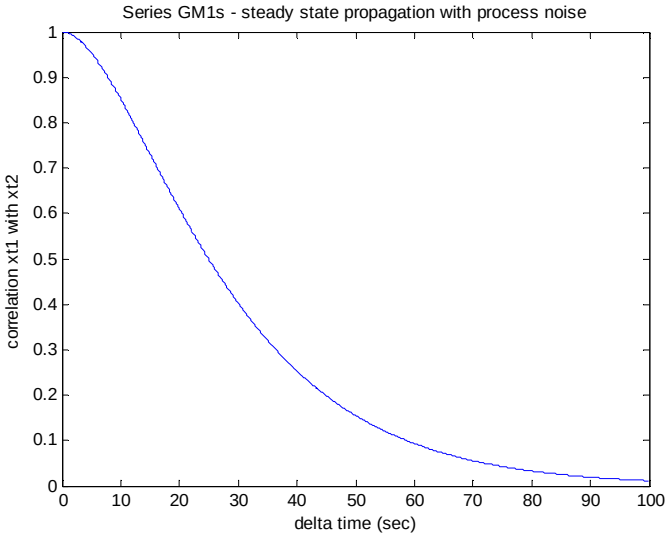

Figure 5. Series GM1 position (auto) correlation.

The other two dynamic models described earlier correspond to non-stationary stochastic processes, as illustrated by position variance (one-sigma) vs. time in Figure 6 ("blue" Series GM1, "green" GM1 Velocity, "red" Integrated Velocity). GM1 Velocity was approximated using Series GM1 and the parameters of Equation 9 except for the value $T_1 = 750$ seconds; Integrated Velocity was approximated similarly with the additional value of $T_2 = 1000$ seconds. Because of their ever increasing position variance as a function of time, these two dynamic models are not suitable for modeling bounded reference trajectory error other than during periods of data drop-out when the error grows. Also, their temporal correlation between position at two different times is generally higher than for the Series GM1 dynamic model. For example, the correlation between position at $t = 10$ seconds and $t = 30$ seconds (delta time = 20 seconds) equals 0.77 for the Integrated Velocity model. It also equals a different value, 0.95, for $t = 40$ seconds and $t = 60$ seconds, since it corresponds to a non-stationary stochastic process.

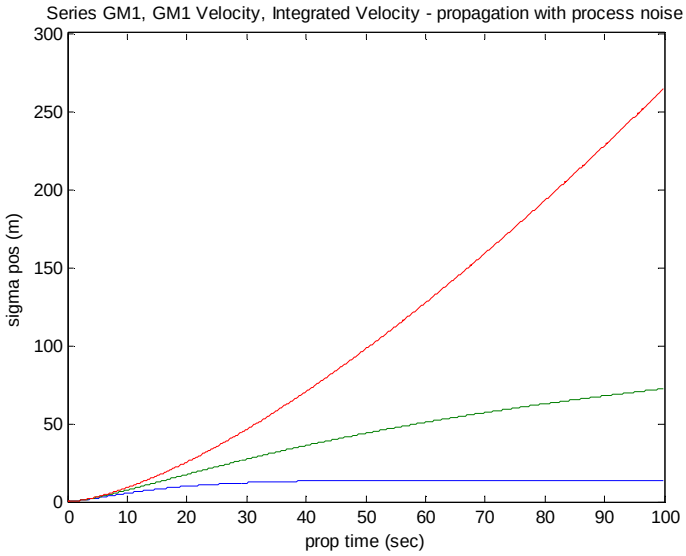

Figure 6. Position error one-sigma vs. time for 3 different dynamic models.

EXAMPLES OF KALMAN FILTER REGISTRATION

A Kalman Filter was implemented based on simulated data and its performance assessed. The data corresponds to the generic sensor/platform imaging scenario depicted in Figure 7 - a "racetrack" trajectory imaging a constant area of interest (AOI) to the East. 8000 overlaying image frames were taken at a 10 hertz rate. Their size is 5k x 5k pixels with a nadir gsd of 0.25 m. Ground points were measured with an image measurement error of 1.0 pixels, one-sigma. An available DEM was simulated with 2 m one-sigma random z error and 1.5 m one-sigma bias z error. Three uncorrelated ground control points were also assumed available with 1m (one-sigma) component error. One loop around the racetrack is completed approximately every 250 seconds.

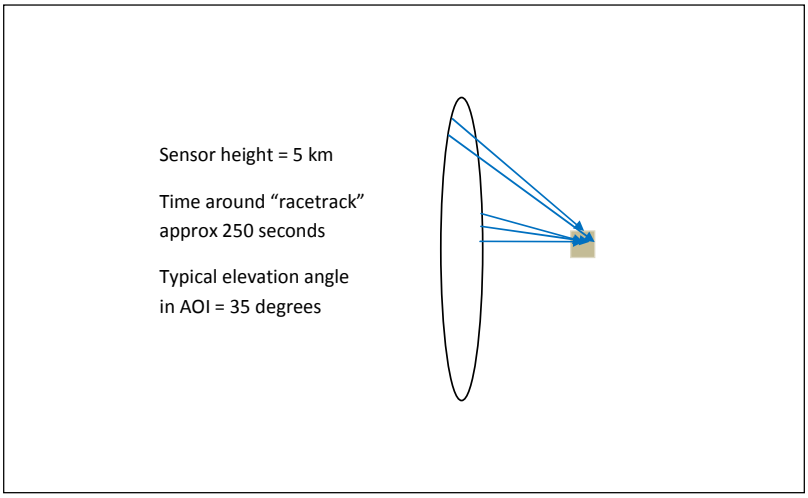

Figure 7. General imaging scenario.

The simulator was written in matlab and consists of four major modules: (1) Simulation Control, (2) Data Generator, (3) Kalman Filter, and (4) Performance Evaluator. The Data Generator generates simulated image measurements of all relevant ground points. It also generates both a true trajectory and the reference trajectory input

in to the Kalman Filter, along with the measurements. The difference between the two trajectories (reference trajectory error) is generated using random numbers consistent with the Series GM1 dynamic model and the parameter values of Equation 9 with initial covariance matrix P_0 set to P_0^* , a diagonal matrix with $15^2\ m^2$ and $1.5^2\ m^2/s^2$ down the diagonal to approximate steady state values. The measurements are then generated by the Data Generator using a sensor model, the true trajectory, and the addition of random measurement error.

The Kalman Filter estimates reference trajectory error (corrections) along with other state vector components at each frame or time t_k. In particular, the Kalman Filter state vector consists of 3 groups of sensor position/velocity components corresponding to along-track, cross-track, and radial coordinates, 3 groups of sensor attitude/rate components corresponding to omega, phi, kappa attitude angles, a DEM z-bias correction for the AOI, and 3D locations for all relevant tie and/or ground control points. In order to estimate the state vector components corresponding to each group of reference trajectory errors, the Kalman Filter also implements an underlying dynamic model via Equations 1, where the Φ and Q are generated using Equations 5 along with the parameters detailing the assumed dynamic model (e.g., Equations 9). The assumed dynamic model is specifiable and can be different than the one used by the Data Generator to generate reference trajectory error.

Results: Kalman Filter "off"

Prior to describing Kalman Filter performance, let us first describe the actual reference trajectory error input in to the Kalman Filter. Figure 8 presents corresponding sensor along-track (x), cross-track (y), and radial (z) position error. (Attitude errors have the same statistics, after scaled appropriately by inverse range.) Note that errors are essentially in steady state and are also within their one-sigma envelopes a reasonable amount of time. Also, errors are positively correlated over time, i.e., errors corresponding to the same component at two different times are typically nearly the same value when the two times are within the same but arbitrary time interval of about 20 seconds or less. This time interval corresponds to a theoretical correlation of 65% or greater - see Figure 5.

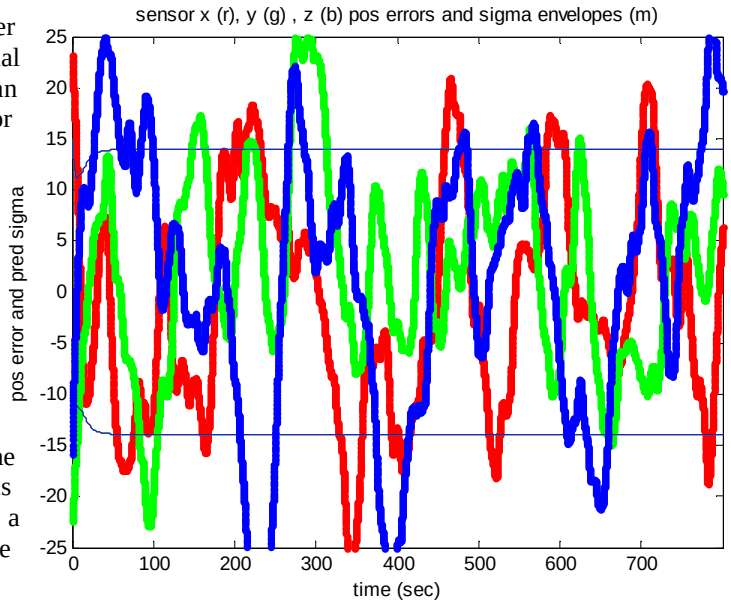

Figure 8. Reference trajectory position errors.

Figure 9 presents monoscopic extraction error assuming that the extraction process uses the uncorrected reference trajectory (no Kalman Filter). Magenta corresponds to CE 90% horizontal accuracy predictions, red to horizontal error, green to LE 90% vertical accuracy predictions, and blue to absolute vertical error. Results were averaged over four different ground points per frame. There were 8000 frames and a total of 32,000 different ground points. Accuracy predictions are based on error propagation, with a primary input consisting of the reference trajectory error covariance (Equations 4) computed corresponding to the Series GM1 dynamic model and the corresponding parameter values of Equation 9 with $P_0 = P_0^*$, i.e., statistically the same model as used to generate the error by the Generator module. Note the general CE oscillatory trend in Figure 9, which corresponds to varying sensor position along the "racetrack".

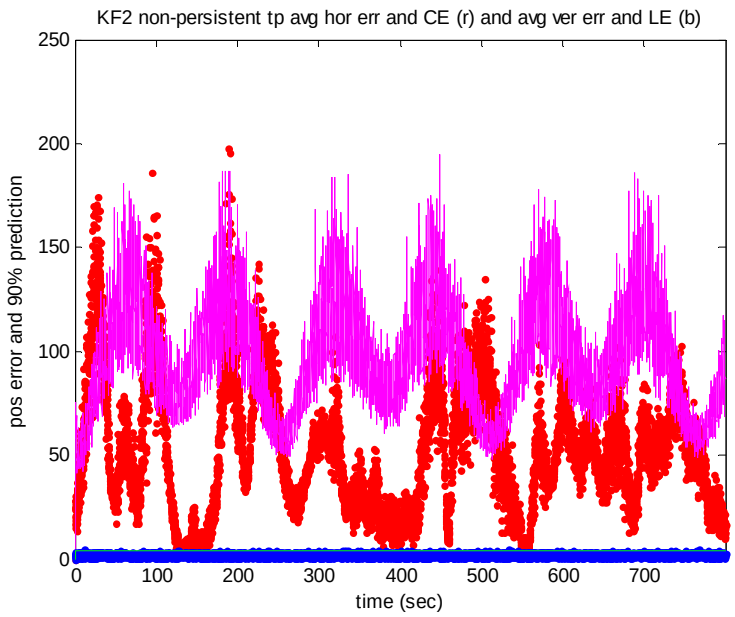

Figure 9. Monoscopic extraction error corresponding to uncorrected reference trajectory.

Results: Kalman Filter "on" with Correct Dynamic Model

Kalman Filter performance is now described. The Kalman Filter utilized measurements from tie points and briefly ground control points. There were 3 tie points, the points measured in each of the 8000 frames. There were 3 control points, but the points were measured in one frame only – frame 6000. (They were included for generality of the experiment, but only near the end of the overall simulation time interval of 800 seconds.) Thus, the Kalman Filter state vector included locations of the 3 tie points and 3 control points.

The first sub-experiment implemented a Kalman Filter which (statistically) implemented the same dynamic model as was used to generate the reference trajectory error, i.e., the Series GM1 using the parameter values of Equation 9 with $P_0 = P_0^*$. That is, for each trajectory group in the state vector, the Kalman Filter prediction equations (Equations 1) implement the state transition matrix Φ and the process noise error covariance matrix Q generated via Equations 5. (Of course, these individual 2×2 Φ and Q are first placed in to the appropriate block diagonal of the larger $n \times n$ Φ and Q.) The remaining state vector elements correspond to tie point locations, control point locations, and DEM z-bias correction. They have state dynamic models and initial error covariance commensurate with static points, very large tie point initial horizontal uncertainty, and control point and DEM uncertainties as described previously. Finally, all trajectory components and ground point components were assumed uncorrelated at t_0.

Kalman Filter results are presented in figures 10 and 11 (note the change in the range of the y-axis). Figure 10 presents tie point solution error as a function of time. Errors were computed by differencing the appropriate components of the Kalman Filter state vector with the true ground point locations computed by the Data Generator. Accuracy predictions were computed from the appropriate portion of the Kalman Filter state vector error covariance.

Figure 11 presents monoscopic extraction results corresponding to four different and arbitrary ground points measured in each frame, for a total of 32,000 different points across the 8000 frames. The monoscopic extractions correspond to a parallel process outside of the Kalman Filter, but are based on the Kalman Filter state vector estimate (corrected reference trajectory) applicable at the time of the corresponding frame, i.e., in "real-time".

Both figures present CE 90% horizontal accuracy predictions based on the Kalman Filter error covariance and error propagation (magenta line), and horizontal errors (red dot). Similarly, LE 90% vertical accuracy predictions (green line) and absolute vertical errors (blue dot) are presented.

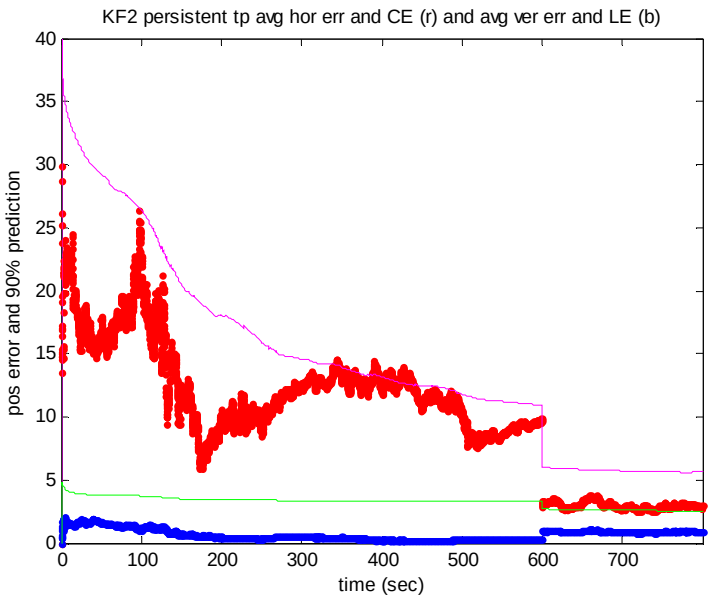

Figure 10. Tie point solution error corresponding to recommended Series GM1 dynamic model.

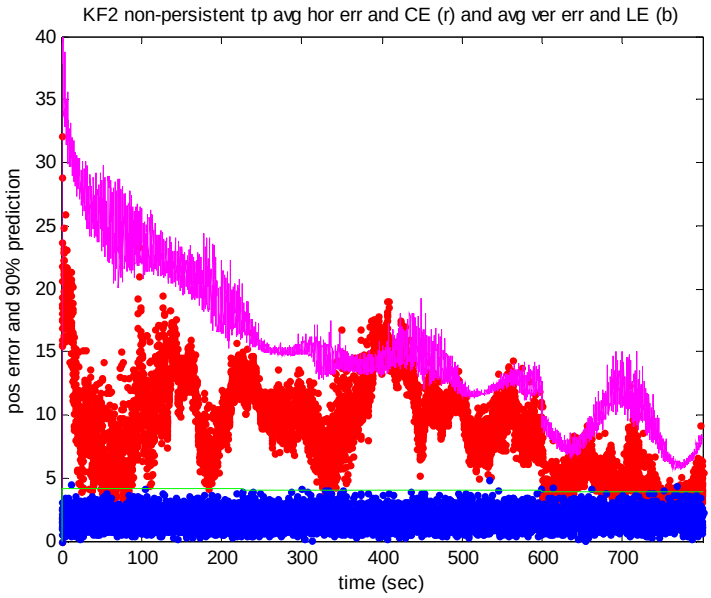

Figure 11. Monoscopic extraction error corresponding to recommended Series GM1 dynamic model.

Note the consistency of actual errors relative to predicted accuracies, and the significant improvement in geo-positioning accuracy due to inclusion of the tie points, i.e., the improvement over time in Figures 10-11. The tie points get more accurate with time due to multiple image rays and changing imaging geometry, and due to the absorption of independent information from the reference trajectory for image frames separated in time on the order of 60 seconds or more, and hence correlated less than 10% - see Figure 5. The tie points essentially become increasingly more accurate "pseudo control points" as time increases, which in turn improve the state estimate for

corrections to the reference trajectory, which in turn improves monoscopic extraction accuracy for arbitrary points in the image frames. Relative to results using the uncorrected reference trajectory (Figure 9), use of the tie points allows for an approximate 10x accuracy improvement at approximately 575 seconds into the overall registration time interval and without the use of ground control.

In addition, even though the tie points were measured in every frame for this sub-experiment, this is not required as long as the same tie points are measured throughout the time period. For example, the sub-experiment was repeated using the same 3 tie points but measured only every 10th frame. Monosocpic extraction results were nearly identical; for example, CE=14 m vs. the previous 12 m at $t = 575$ seconds. However, when measured only every 50th frame, accuracy started to degrade significantly; for example, CE=23 m vs. the previous 12 m at $t = 575$.

(Note that all accuracies addressed in this paper are absolute accuracies; although with the inclusion of tie points, relative accuracy should improve significantly as well for points extracted in different frames.)

Results: Kalman Filter "on" with Incorrect Dynamic Model

The second sub-experiment was identical to the first, i.e., the same measurements and reference trajectory. However, the Kalman Filter implemented the Integrated Velocity dynamic model instead of the Series GM1 model. (The Integrated Velocity model was approximated by the Series GM1 and Equation 9 but with $T_1 = 750$ and $T_2 = 1000$ seconds). As can be seen in Figures 12 and 13, consistency of actual errors relative to predicted accuracies was marginal, and both errors and predicted accuracies larger (worse) than in Figures 10-11. However, the additional availability of ground control points (frame 6000) did mitigate these adverse effects.

(A second set of sub-experiments was also performed, identical to the two sub-experiments described previously except that there were no tie points and the control points were measured every 200th frame. Typical monoscopic extraction results were CE=45 m using Series GM1 and CE= 95 m using Integrated Velocity, with errors reasonably consistent with accuracy predictions for both sub-experiments. The relatively long time interval between control updates coupled with large variance growth across this time interval with the Integrated Velocity dynamic model yield inferior results relative to the Series GM1 dynamic model.)

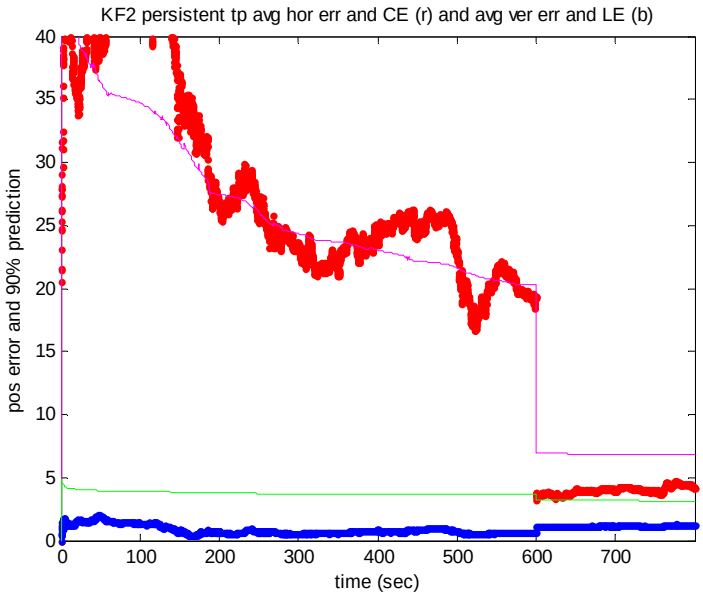

Figure 12. Tie point solution error corresponding to Integrated Velocity dynamic model.

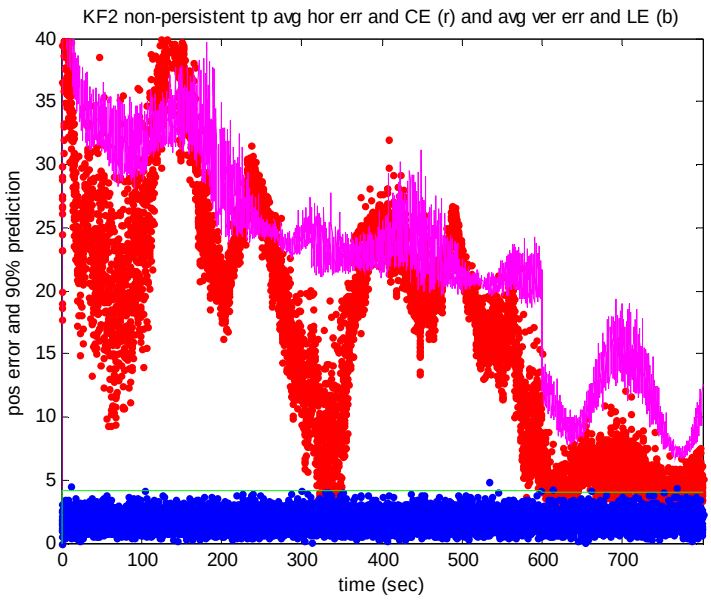

Figure 13. Monoscopic extraction error corresponding to Integrated Velocity dynamic model.

Operational Issues

As described above, use of the Serial GM1 dynamic model in the generic scenario of interest yields impressive geopositioning performance. However, there are two issues that need to be addressed for an actual implementation in an operational scenario. First, the appropriate parameters detailing the dynamic model (e.g., Equation 9) must be reasonably estimated by analysis of corresponding sensor/platform requirements/design documents, and/or tuning of the parameter values based on operational data and comparison of corresponding extraction results to ground truth. Second, it is recommended that the corresponding Kalman Filter also contain various "real-world" design features, including the monitoring of measurement residuals in order to detect any non-obvious meta-data drop-out or unexpected degradation of *a priori* meta-data accuracy. If detected and in order to mitigate their adverse effects, the Kalman Filter can temporarily increase the value of the process noise matrix Q by its multiplication by a scalar $s > 1$, or even temporarily switch to one of the other dynamic models with increasing error variance.

SUMMARY

A Kalman Filter for the registration of video frames was presented. In particular, an underlying dynamic model of reference trajectory error was described and recommended for optimal Kalman Filter and subsequent geopositioning performance. This dynamic model, the Series GM1 model, is implemented as part of the Kalman Filter and captures the assumed statistical characteristics of reference trajectory error – bounded with relatively constant expected magnitude and temporal correlation characteristics. The Kalman Filter then corrects the reference trajectory based on measurements from a combination of ground points measured in the video frames.

Detailed examples of registration performance were then presented based on simulated data. The overall scenario corresponds to a generic sensor/platform in a "racetrack" trajectory at a height of 5 km imaging a constant area-of-interest to the East. 8000 sequential and overlaying video frames cover the area-of-interest. Corresponding analysis demonstrated the superiority of the recommended dynamic model for this application over the more usual dynamic models employed by the tracking community. It also demonstrated the important role that tie points play in overall registration performance. In particular, tie points alone in conjunction with the Kalman Filter and recommended dynamic model, provide for an approximate 10x improvement in geopositioning accuracy relative to monoscopic extraction accuracy using the uncorrected reference trajectory.

APPENDIX

The transition matrices and process noise covariance matrices for the various dynamic models were derived by the author using the following fundamental equations from linear systems theory. The equations correspond to a continuous linear time invariant system and results were then discretized accordingly. See (Gelb, 1974) and (Bar-Shalom, 1988) for further details.

$$\dot{X} = FX + W$$

$$X(t) = \Phi(t, t_0)X(t_0) + \int_{t_0}^{t} \Phi(t, \tau)W(\tau)d\tau$$

$E\{W(\tau_1)W^T(\tau_2)\} = \Gamma\delta(\tau_1 - \tau_2)$, where δ is the dirac delta function

$\Phi(\mathrm{t}, \mathrm{t}_0) = \Phi(\mathrm{t} - \mathrm{t}_0) = \Phi(\Delta\mathrm{t}) = \mathcal{L}^{-1}\{(\mathrm{sI} - \mathrm{F})^{-1}\}$, where $\mathcal{L}^{-1}$ is the inverse Laplace transform

$Q(\Delta t) = E\{X(\Delta t)X^T(\Delta t)\}$, where $t_0 = 0$, $t = \Delta t$, and $X(t_0) = 0$

$$Q(\Delta t) = \int_0^{\Delta t} \Phi(\Delta t - \tau)\Gamma\Phi^T(\Delta\mathrm{t} - \tau)\mathrm{d}\tau$$

$E\{X(t)X^T(t + \Delta t)\} = \int_{-\infty}^{t} \Phi(t - \tau)\Gamma\Phi^T(t + \Delta t - \tau)d\tau$, in steady state and assuming a stable system.

REFERENCES

Bar-Shalom,Yaakov and Thomas Fortmann (1988). *Tracking and Data Association*, Academic Press.

Gelb, Arthur (1974). *Applied Optimal Estimation*, MIT Press.

Taylor, Charles R., John T. Dolloff, Matt Bower, Scott B. Miller (2010). "Automated Video Georegistration at Real-Time Rate", *Proceedings from the ASPRS Annual Conference*, San Diego, CA, April 26-April 30, 2010.

Approved for Public Release: Case #11-097